In situ Monitoring of Wet Granulation Using Online X-Ray Powder Diffraction

Tiffani D. Davis,[1] Kenneth R. Morris,[1,4] Huapeng Huang,[2] Garnet E. Peck,[1] Joseph G. Stowell,[1] Bradley J. Eisenhauer,[3] Jon L. Hilden,[1] David Gibson,[2] and Stephen R. Byrn[1]

Received July 21, 2003; accepted August 1, 2003

Purpose. Polymorphic transformations during the wet granulation of a metastable polymorph of flufenamic acid were monitored *in situ* using online X-ray powder diffraction. The resulting data were used in testing a proposed process induced transformation rate model, which allows the extent and occurrence of polymorphic transformations during wet granulation to be controlled by adjusting the granulation time.

Methods. A small-scale, top mixing granulator was designed for compatibility with novel X-ray powder diffraction equipment (available from X-Ray Optical Systems of East Greenbush, NY).

Results. The unique polycapillary optic and X-ray source allowed the transformation of the metastable to the stable polymorph to be followed during the granulation. Following a diffraction peak each for the metastable and stable forms demonstrated that polymorphic transformations during the wetting phase of granulation follow the trends predicted by the model.

Conclusions. The advanced online monitoring may allow real-time control of the process by the adjustment of process parameters, such as granulation time, and clearly qualifies as a PAT (process analytical technology).

KEY WORDS: wet granulation; polymorphism; flufenamic acid; online x-ray powder diffraction; process analytical technology (PAT)

INTRODUCTION

Wet granulation is a size enlargement process during which small particles are combined with a binder to form larger, physically strong agglomerates (1). During wet granulation, a solvent, usually with a polymeric binder, is added to wet the drug substance and excipients. A potential liability of the wet granulation process is that the addition of solvent and subsequent dissolution of the drug substance can facilitate a transformation to alternate crystalline forms (2–5).

Although X-ray powder diffraction is the "gold standard" in the quantification of crystalline forms, online X-ray quantitative powder diffraction of pharmaceuticals has only been reported once in the literature. MacCalman, *et al.* (6) used online X-ray powder diffraction for the analysis of polymorphic forms of an antibiotic during the crystallization of an active pharmaceutical ingredient. The crystallized slurry was pumped through the online crystallization system, while X-ray powder diffraction patterns were recorded *in situ* through mica windows to analyze the conversion of solvate C to solvate A. There are no reports, however, of on-line X-ray powder diffraction monitoring of a secondary pharmaceutical operation. Emerging non-pharmaceutical uses of online X-ray powder diffraction include the monitoring of cement components for quality control (7,8), the monitoring of gypsum during wall board manufacturing (9), as well as the reactivity of catalysts (10–13).

A prototype X-ray powder diffraction instrument (X-Ray Optical Systems, East Greenbush, NY) was adapted for the purposes of this study. This instrument uses parallel beam polycapillary optics to both alleviate artifacts and "amplify" the low power source to obtain a high X-ray flux (14,15). The polycapillary optic consists of 10,000 to several million hollow glass channels bundled together. The X-rays propagate through the capillary by total reflection at the glass surface, which is accomplished by decreasing the angle of incidence of the X-ray beam to less than some critical value. For Cu Kα radiation used in the current work, the critical angle is 0.22°. Polycapillary optics can be used in both focusing and collimating modes to direct the X-ray beam. The collimating polycapillary optic converts diverging X-rays into a quasi-parallel beam. This parallel-beam geometry greatly reduces or removes many of the sources of error commonly seen in the more commonly used parafocusing geometry, such as flat specimen, displacement, and specimen transparency error. The elimination of these sources of error, and the potential for using reduced power systems, makes parallel beam X-ray systems well suited for online diffraction (15).

The model compound chosen was flufenamic acid (FFA) (Fig. 1). Flufenamic acid is a potent anti-inflammatory agent used in the treatment of rheumatoid arthritis, osteoarthritis, and pain. It is known to exist in at least six polymorphic forms, with forms I and III most extensively studied. Forms I and III are enantiotropically related, with form III being the stable form below the transition temperature of 42°C, and form I being stable above 42°C (16). Unpublished data collected in our laboratory has demonstrated a polymorphic conversion of the metastable form I to the stable form III during wet granulations with ethanol. This is easily observed visually, as the metastable form I exits as a white powder, and the stable form III exits as a yellow powder. Quantification of the

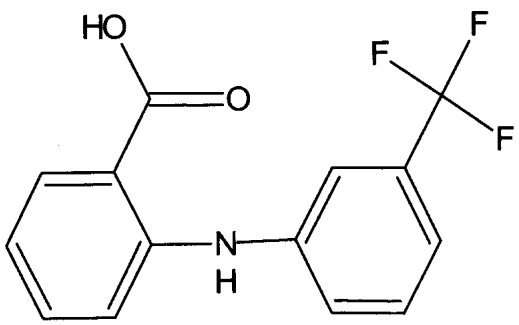

Fig. 1. Structure of flufenamic acid.

[1] Department of Industrial and Physical Pharmacy R. E. Heine Building, 575 Stadium Mall Drive, Purdue University, West Lafayette, IN 47907-1336.

[2] X-Ray Optical Systems, Inc., 15 Tech Valley Drive, East Greenbush, NY 12061.

[3] Department of Chemical Engineering, Chemical Engineering Building, 480 Stadium Mall Drive, Purdue University, West Lafayette, IN 47907-2050.

[4] To Whom correspondence should be addressed. (e-mail: morriskr@purdue.edu)

polymorphic forms using offline X-ray powder diffraction was highly problematic, because the transformation occurred simultaneously with ethanol evaporation. Therefore, an online method was required to study this transformation.

The purpose of this article is two-fold: To demonstrate the use of online X-ray powder diffraction for the first time in a pharmaceutical secondary unit operation, and to use the online data for testing a proposed model for polymorphic transformations during the wetting phase of granulation.

MATERIALS AND METHODS

Materials

Microcrystalline cellulose (MCC) (PH 102, Lot No. 2521) was obtained from F.M.C. of Newark, Delaware. Flufenamic acid (lot # LI 04731KI) was acquired from Aldrich of Milwaukee, WI.

Preparation and Characterization of Polymorphs

Flufenamic acid form I was produced by placing flufenamic acid as received from Aldrich in an 85°C oven overnight. The crystals were then milled in a Janke and Kunkel grinder (Janke and Kunkel KG, Germany) and sieved using a Ro-Tap (Model RX-29, W.S. Tyler, Mentor, OH), and only those crystals passing through the 90 μm sieve were used for granulations and analysis.

Flufenamic form III was obtained by re-crystallization from ethanol at twice the saturation solubility at 25°C. The flufenamic acid/ethanol solution was heated to approximately 60°C to dissolve all of the flufenamic acid, and then cooled to room temperature with constant agitation. The resulting crystals were separated by vacuum filtration, and then sieved using a Ro-Tap. Only crystals smaller than 90 μm were used for analysis.

Phase identification and purity of all polymorphs was assessed using X-ray powder diffraction and comparison with the calculated pattern. The calculated XRPD patterns were generated using Cerius^2 ™ software from the corresponding single-crystal structures obtained from the Cambridge Structural Database (refcode: FPAMCA for form III, and FPAMCA11 for form I).

Preparation of Calibration Samples

Physical mixtures of flufenamic acid polymorphs were prepared by weight using a four-place analytical balance (Model AG 104, Mettler Toledo Inc., Switzerland). Calibration samples were prepared using a ternary mixture of flufenamic acid forms I and III in microcrystalline cellulose. All calibration samples were diluted with 50% microcrystalline cellulose, and consisted of 0%, 5%, 10%, 15%, 25%, 40%, and 50% form I in the total mixture. (For instance, samples denoted as 25% form I contained 25% form I, 25% form III, and 50% microcrystalline cellulose.) A total sample weight of 1.5 g was used, and all samples were prepared by geometric mixing of the sieved crystals. Although thorough mixing was assumed, it could not be completely assured, because form I exists as a prism, and form III as a needle (16). The samples were placed in a sample holder that would fit inside the mixing bowl, and equipped with a small sample cell (3.5 cm long by 1.9 cm wide, and 4 mm deep) at the height of the Mylar window. This avoided using inordinate amounts of material for the generation of the calibration curve, while also obtaining X-ray powder diffraction patterns inside the mixing bowl. The calibration curves displayed good linearity, with a correlation coefficient of 0.9255 for form III and 0.9769 for form I.

To account for the different conditions between the calibration samples and granulation samples, the peak heights for the granulation samples had to be related to the calibration peak heights. This was accomplished by generating a second calibration curve using the peak heights of two samples of known content from all three granulations. The two samples consisted of 0% form I and 50% form I. (Because linearity was established with the calibration samples, two points were considered suitable for generating a second calibration curve.) It was assumed that the final material consisted of 50% form I and the transformation was complete. If the final readings of the granulation began to plateau, the average peak height was calculated for all data points after and inclusive of the maximum reading.

Wet Granulations

Flufenamic acid wet granulations were completed in triplicate and consisted of 50% flufenamic acid form I and 50% microcrystalline cellulose with a total load size of 124 g. Ethanol (approximately 18% w/w) was used as the granulating liquid at a flow rate of 5 mL/min, and was added within the first 7 minutes of the granulation by a peristaltic pump. The granulation was run for approximately 2 hours with constant XRPD monitoring.

X-Ray Powder Diffraction (XRPD)

The online powder patterns were obtained using CuKα radiation with a 40kV/1mA (40W) Oxford 5011 source and monolithic polycapillary collimating optic with 30 mm input focal distance and 6 mm bundle size. An Amptek XR-100CR Si X-ray detector, and SIEMENS goniometer table were used for X-ray analysis. All granulations were analyzed in step mode, from 17–37° 2θ using a 1 s acquisition time. For X-ray analysis, the granulator was placed off-center in reference to the diffraction table as shown in Fig. 2. This allows the X-ray beam to penetrate the Mylar window at a glancing angle, and avoid large sample absorbance. The X-rays entered the

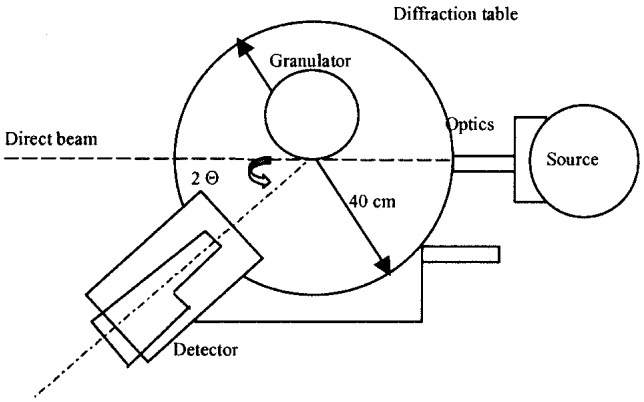

Fig. 2. Schematic drawing showing top view of X-ray diffractometer and granulator.

granulator and the diffracted radiation was collected by the detector at the 2θ angle.

Due to the constraints of the small sample X-ray holder (described in the preparation of the calibration samples), preferred orientation could not be avoided. However, good linearity was observed for the X-ray powder diffraction calibration curves.

The offline X-ray diffraction powder patterns for the control granulation were obtained on a Shimadzu XRD-6000 X-ray diffractometer (Kratos Analytical, Chestnut Ridge, NJ). Diffraction patterns were collected using Cu Kα radiation, over the range of 10°-40° 2θ, at a rate of 4° 2θ per minute with a step size of 0.04° (40kV, 40mA).

All X-ray powder diffractograms were analyzed using GRAMS32 AI software (Version 6, Galactic Industries Corporation, Salem, NH). For the quantitation of form I, the absolute peak height in counts was used, whereas peak height after baseline subtraction was used for the quantitation of form III. The peak height was determined by finding the highest intensity in the peak range (24.1–24.9° 2θ for form I, and 34.8–35.8 ° 2θ for form III). The average intensity between 35.8–36° 2θ was used as the baseline for the quantitation of form III.

Equipment

The granulator was designed at Purdue University to be compatible with the online X-ray powder diffraction equipment. A high torque mixer (Stir-Pak, Cole-Parmer Instrument Co., Vernon Hills, IL) was used for overhead mixing, and a modified mixing bowl was designed for small-scale granulations. The mixing bowl was 7.5 cm in diameter and 14.5 cm deep, with a 600 mL capacity. In order for the X-ray beam to penetrate into the mixer, a window 2 cm tall, spanning half the circumference, was covered with 25 μm Mylar (Chemplex Industries, Inc., Palm City, FL), because Mylar is transparent to X-rays. A mixing blade designed for semisolids, (Cole-Parmer Instument Co., Vernon Hills, IL) which allows 1/8 inch clearance between the blade and the bowl was installed, and facilitated the necessary movement of the powder by the window, while producing the agitation needed for granulation. For compatibility with the X-ray instrument, a bottom plate was added to hold the mixing bowl above the goniometer table, and a support was added to secure the mixing bowl during the granulations.

Solubility

The solubility of flufenamic acid form III in ethanol at 25°C was determined in triplicate by UV spectroscopy on a Cary 50 Bio UV-Vis Spectrophotometer (Varian, Australia) at 288 nm.

The solubility of the metastable form I was estimated at 25°C from the intrinsic dissolution rates (17) of flufenamic acid form I and form III under sink conditions and from the measured equilibrium solubility of form III. The solubility was then estimated by using Eq. 1:

$$Cs_I = \frac{(dC_I/dt)}{(dC_{III}/dt)} Cs_{III} \quad (1)$$

where Cs_I is the estimated solubility of form I, dC_I/dt is the intrinsic dissolution rate of form I, dC_{III}/dt is the intrinsic dissolution rate of form III, and Cs_{III} is the equilibrium solubility of form III at 25°C. The solubility of form III was determined from the plateau concentration following crystallization, and was found to be 336.3 ± 7 mg/mL. Because the ratio of the intrinsic dissolution rates was found to be 2.59, the estimated solubility of form I at 25°C is approximately 871 mg/mL.

For the measurement of the intrinsic dissolution rates, 400–450 mg of material was compressed into a 0.9 cm modified tablet die, using a force of 1000 lbs with a 12 s dwell time on a Carver press (Fred S. Carver, Inc., Summit, NJ). All aliquots taken during dissolution were analyzed by UV spectroscopy at 288 nm using a Beckman DU-7 Spectrophotometer (Irvine, CA). To ensure no polymorphic conversion occurred as a result of compaction, X-ray powder diffraction was run before and after compaction for both polymorphs. No changes in the diffraction pattern were observed following compaction indicating no polymorphic conversion. Although the metastable form I may transform to the stable form III by means of a solution mediated conversion at the surface of the disk, an X-ray powder diffraction pattern was obtained after 3 min dissolution. This time frame was chosen in order to have adequate material for an X-ray powder diffraction pattern. No changes in the diffraction pattern were observed following dissolution. The time interval chosen for the acquisition of the intrinsic dissolution rate of form I was therefore 3 min.

Surface Area Analysis

The surface area of flufenamic acid form I and microcrystalline cellulose was measured in triplicate with a Micromeritics ASAP surface area analyzer (Micromeritics, Norcross, GA), using nitrogen gas as the adsorbate and applying the BET equation. The surface area of flufenamic acid form I and microcrystalline cellulose was found to be 0.8818 ± 0.031 m^2g^{-1} (r^2 = 0.9996 ± 0.0001) and 1.659 ± 0.143 m^2g^{-1} (r^2 = 0.9999 ± 0.0001), respectively.

Growth Rate Constant

The growth rate constant for flufenamic acid was determined by analyzing the desupersaturation profile at 25°C. A 300 mL jacketed beaker connected to a Neslab RTE-111 water bath (Newington, NH) was used to control the temperature of the solution. A supersaturated solution, with a concentration between the solubility of the metastable and stable polymorphs (approximately 375 mg/mL) was prepared. Once crystallization was observed, a timer was started to determine the concentration and hence the amount crystallized at each time point. The supersaturated solution was analyzed by UV spectroscopy at 288 nm using a Cary 50 UV spectrophotometer (Varian, Australia).

Determination of Ethanol Available from Microcrystalline Cellulose

The volume of ethanol available for dissolution of flufenamic acid was determined by calculating the ethanol content corresponding to the end of the heat transfer (evaporative) stage of drying. This amount represents the "free" ethanol on the surface of a granule (18). Drying curves for three ethanol-wetted samples of microcrystalline cellulose were obtained, and the point at which the drying process changed

from linear to exponential (evaporative to diffusion limited) was found by using a point-by-point linear regression on the appropriate equation until the correlation coefficient starts to decrease. From the point-by-point regression, the percentage free ethanol was found to be 48.267% ± 1.39%, which corresponds to 17 mL ethanol.

Modeling and Data Fitting

The model described in the background and theory section was derived and committed to code (C#) to simulate the processes in the granulation. The computer modeling focuses on the calculation of the concentration values, with m_I and m_{III} values being byproducts of this process. An iterative approach is used to approximate and refine the changes in these values over a series of finite time intervals.

For each time interval (0.01 min), the initial mass of form I, m_{Ii}, mass of form III, m_{IIIi}, concentration, C_i, are all known, and initial rate of change in concentration $(dc/dt)_i$ is calculated by the following:

$$\frac{dC}{dt} = -\frac{\frac{dm_I}{dt} + \frac{dm_{III}}{dt}}{V} \tag{2}$$

in which V is the volume of granulating liquid free to dissolve the flufenamic acid, and the other variables are as previously defined. Assuming constant dm_I/dt and dm_{III}/dt over the time interval, initial estimates for m_{If} and m_{IIIf} are calculated. From these values, the final concentration, C_f, and final rate of change in concentration $(dC/dt)_f$ were calculated from Eq. 3.

$$C = \frac{(m_{Io} + m_{IIIo} + C_o V) - (m_I - m_{III})}{V} \tag{3}$$

Although concentration is an unknown function with respect to time, an approximation needs to be made over each time interval. For simplicity, a constant second derivative over each interval was assumed. This yields:

$$C(t) = C_i + \left(\frac{dC}{dt}\right)_i t + \frac{1}{2}\left(\frac{d^2C}{dt^2}\right)t^2 \tag{4}$$

The second derivative of concentration was obtained from $(dC/dt)_i$ and the initial estimate of $(dC/dt)_f$. Substituting Eq. 4 into either Eq. 7 or Eq. 9, and integrating allows us to express m_{If} and m_{IIIf} over the time interval as

$$\Delta m_I = k_{DS}\left[Cs_I\Delta t - \left(C_i\Delta t + \frac{1}{2}\left(\frac{dC}{dt}\right)_i \Delta t^2 + \frac{1}{6}\left(\frac{d^2C}{dt^2}\right)\Delta t^3\right)\right] \tag{5}$$

and

$$\Delta m_{III} = k_G\left[Cs_{III}\Delta t - \left(C_i\Delta t + \frac{1}{2}\left(\frac{dC}{dt}\right)_i \Delta t^2 + \frac{1}{6}\left(\frac{d^2C}{dt^2}\right)\Delta t^3\right)\right] \tag{6}$$

From the new values, C_f can be recalculated using Eq. 3. If the value obtained for C_f differs from the previous value by more than 0.00001, the process is repeated using the new m_{If}, m_{IIIf}, and C_f values. Final values from this interval are then used as initial values for the next interval.

Data fitting for the dissolution rate constant was performed using a least squares method.

RESULTS AND DISCUSSION

Wet Granulation Analysis

Figure 3 shows a representative waterfall plot of the diffractograms for one of the flufenamic acid granulations (granulation 1). Although several of the reflections could have been chosen for analysis, the (30-2) peak, indicative of form I, and both the (314) and (202) peaks, indicative of form III, were used to follow the transformation because they are relatively well resolved. The amorphous scattering observed in all X-ray powder diffraction patterns is from microcrystalline cellulose. As the granulation progresses, the (30-2) peak at 24° 2θ, indicative of form I, decreases in area and intensity, while the form III peaks, (314) and (212), at 35° 2θ increase. By peak height analysis, each time point was converted to the percent polymorph present. Because the collection of the entire diffractogram took approximately 13 min, a 7-min lag time existed between the acquisition of the form I peak at 24° 2θ and form III peaks at 35° 2θ. The time points were therefore corrected for this difference. For simplicity, it was assumed the diffraction peak at 24° 2θ for the first diffractogram occurred at the beginning of the granulation, whereas the peak at 35° 2θ occurred after approximately seven minutes. This time difference was carried through for the analysis of the subsequent diffractograms.

The percent polymorph conversion for a representative granulation (granulation 3) is shown in Fig. 4. The addition of ethanol and subsequent changes in the material (dissolution and densification of the material) may result in outliers for the initial time points. For instance, a very large peak height was observed for the first diffractogram from granulation 3 (138% form I), and was omitted, as it was likely the result of preferred orientation induced by the wetting and densification of the material. Granulation 3 also displayed slightly more interference from the Mylar window and exhibited more noise than granulation 1 (not shown), and therefore exhibits slightly more scatter in the data. Granulation 2 (not

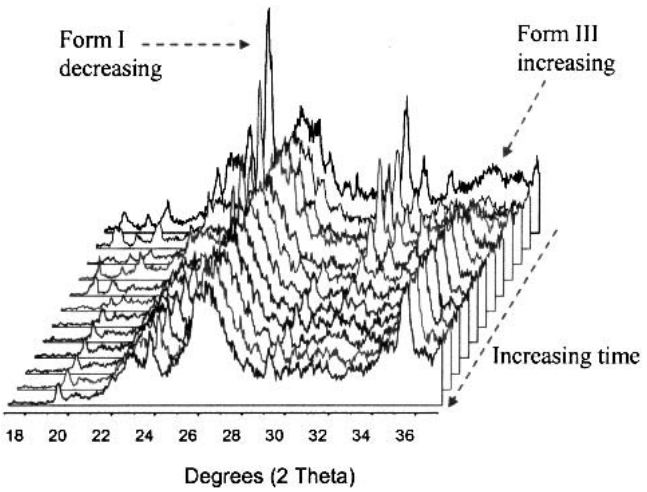

Fig. 3. Waterfall plot of the diffractograms for a flufenamic acid granulation. The peak at 24°, indicative of form I decreases while the peak at 35°, indicative of form III increases with time.

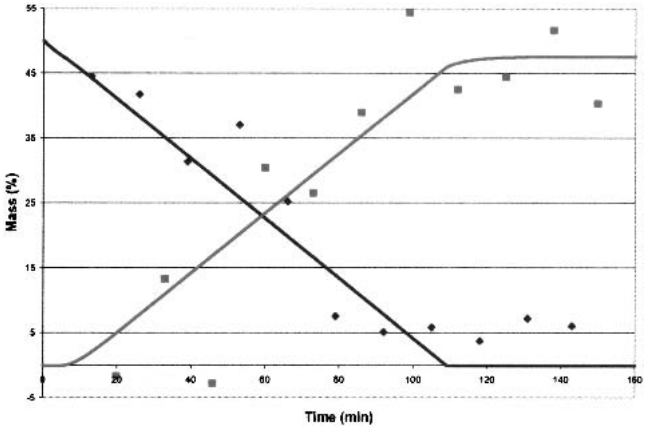

Fig. 4. Peak height analysis with curves predicted from the model for Granulation 3 (Peak height was transformed into mass percent using the calibration curve.) Diamonds represent form I. Squares represent form III.

shown) exhibited a faster conversion than either granulation 1 or 3, because a small amount of ethanol left in the tubing to the granulator was delivered to the mixture prior to the start of X-ray analysis. Granulations 2 and 3 were also briefly interrupted during the online analysis to help clear the Mylar window. Therefore the data just prior to the interruption may not be as representative of the entire material as immediately after. These differences should average out to yield a realistic overall profile.

As seen in Fig. 4, the metastable form I decreases because of its dissolution in ethanol. After dissolution of the metastable form, the stable form emerges and the amount increases due to its nucleation and growth. A lag time between the loss of the metastable form and growth of the stable form is also apparent. This lag time is a result of the time required for metastable form to become supersaturated with respect to the stable form, and for the subsequent nucleation of the stable form as discussed in the theory section. Once supersaturation and nucleation occurred, the stable form continued to grow at a characteristic rate.

To ensure the polymorphic conversion was not a result of the mixing conditions within the granulator, flufenamic acid form I and microcrystalline cellulose were mixed without ethanol for 150 min. Offline XRPD analysis was completed and showed no increase over baseline of form III (not shown).

Modeling of Polymorphic Transformations During Granulation

Metastable polymorphs in a wet granulation may convert to the stable form by means of a solvent-mediated system. In a solution supersaturated with respect to both metastable and stable phases, either one or both phases may crystallize. However, the metastable phase is often initially observed. In solution chemistry, people have attributed the initial observation of the metastable phase to Ostwald's "rule of stages", which states that "an unstable system does not necessarily transform directly into the most stable state, but into one which most closely resembles its own." (19) When the metastable phase crystallizes, the solution concentration decreases until it reaches the solubility of the metastable phase. Throughout this process, the solution is continuously supersaturated with respect to the stable phase. Even though the metastable phase is the major solid component, supersaturation with respect to the stable polymorph may result in the formation of nuclei of the thermodynamically stable phase. It is the formation of nuclei of the stable form that begins the solvent-mediated phase transformation. As the nuclei continue to grow, the solution composition falls toward the solubility of the stable form. This causes the solution to become under-saturated with respect to the metastable phase. Hence, the metastable crystals dissolve and maintain supersaturation and growth of the stable phase. The solvent-mediated phase transformation is complete when all of the metastable phase has disappeared (20).

A conceptual model for solution-mediated transformations during wet granulation follows the rationale of Cardew and Davey (20), and is shown in Fig. 5. The metastable polymorph will go into solution according to its dissolution rate constant, k_{DS}, its solubility and volume of granulating liquid, and will follow Eq. 7.

$$\frac{dm_I}{dt} = -k_{DS}\,(Cs_I - C) = k_{DS}\,(C - Cs_I) \tag{7}$$

The loss of the mass of the metastable form I is (dm_I/dt), where k_{DS} is as defined above, Cs_I is the solubility of the metastable form, and C is the concentration in solution. The dissolution rate constant includes the surface area, A, the diffusion coefficient, D, and the thickness, of the diffusion layer, h, and can be represented by Eq. 8.

$$k_{DS} = \frac{DA}{h} \tag{8}$$

Given enough time, a sufficient amount of the metastable form will have dissolved to produce a supersaturated solution with respect to the less soluble stable form. Assuming rapid nucleation (relative to the granulation time) from the nucleation sites available on the excipients and metastable phase, the stable polymorph begins to crystallize with a growth rate constant, k_G. The growth of the stable polymorph will follow

$$\frac{dm_{III}}{dt} = k_G\,(C - Cs_{III}) \tag{9}$$

where dm_{III}/dt is the change in mass of the stable form III, k_G is the growth rate constant, and Cs_{III} is the solubility of the stable form, and C is as previously defined. Because this process is thermodynamically driven by the solubility differences of the metastable and stable forms, it is not expected to result in a transformation from the stable to the metastable against the thermodynamic gradient.

From the model, a schematic growth curve shown in Fig. 6 was generated. A lag time until the drug exceeds the solubility of the stable form should be observed. When the supersaturation with respect to the stable form is sufficient, the

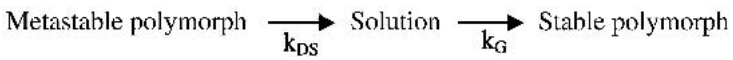

Fig. 5. Conceptual model for solution-mediated phase transformations during wet granulation.

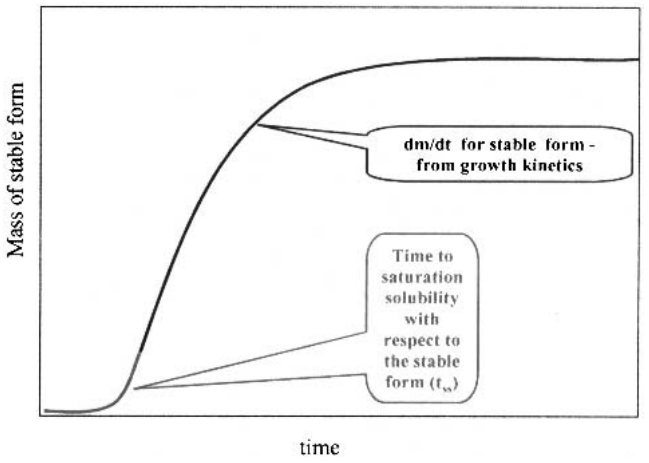

Fig. 6. Schematic growth curve for crystallization during granulation of a metastable form with conversion to the stable form.

mass of the stable form will gradually increase until all of the metastable form has converted to the stable form or the granulation is terminated by drying. Assuming no loss of granulating liquid during the process, all of the material exceeding the solubility of the stable form will convert to the stable form given a sufficient period of time.

To test the model, the online X-ray data were combined with the other constants that were determined separately. This necessitated the determination of the solubilities of both forms, and the growth rate constant and dissolution rate constant. The equilibrium solubility of the stable form at 25°C was found to be approximately 336.3 ± 6.8 mg/mL. Using the intrinsic dissolution rates as described in the experimental section, the solubility of the metastable form was estimated to be 871.0 mg/mL at 25°C. The growth rate constant was determined by analysis of the concentration in solution during the crystallization of the stable polymorph. Knowing the initial concentration and the concentration at each time point, the amount of flufenamic acid crystallized was determined. The growth rate constant was then determined using the slope of the linear fit to the amount crystallized with time, (dm_{III}/dt = 44.3 mg/min), and the solubility of the stable form, (Cs_{III} = 336.6 mg/mL), and the average concentration observed during the crystallization (C ≈ 353 mg/mL). Substituting those values into the growth rate equation (Eq. 9), and solving for k_G, a growth rate constant of 2.6 $cm^3 min^{-1}$ was calculated. The dissolution rate constant could not be obtained from surrogate methods and therefore was obtained by fitting the X-ray data.

From the measured and known amounts, and fitting the dissolution rate constant from the X-ray data, the predicted curves for granulation 3 are shown in Fig. 4. The first point was left out for fitting the granulations (as discussed earlier). Reasonable fit was observed for granulation 1 (not shown), whereas granulation 3 displayed an excellent fit between the data and curves predicted from the model. The differences between the data and predicted curve for the granulation is likely the result of error associated in obtaining online data with this prototype system. For instance, if a constant renewal of material past the Mylar window were not achieved, the X-ray analysis wouldn't be representative of the entire material, and hence would result in larger or smaller values than predicted by the model. Other sources of error include possible interference from the Mylar window and the mixing blade. However, even with the differences between the data and the predicted curves, it is apparent that the general trend of the data follows the model.

The usefulness of this model is the potential for predicting the length of the granulation time required for minimal to no polymorph conversion, partial polymorph conversion, or full polymorph conversion. Thus, when wet granulating with a metastable polymorph, once the solution exceeds the solubility of the stable form, the length of the granulation time will dictate the extent of conversion. If full conversion is desired, the granulation should be continued until the solution mediated conversion is complete. Conversely, if minimal conversion is preferred, the granulation should be stopped either before the concentration exceeds the solubility of the stable form or shortly thereafter. Most importantly, using both the model and advanced online monitoring, such as X-ray powder diffraction, real-time control of the process could be accomplished to control of the polymorphic forms throughout the entire process, as specified by ICH Q6A guidelines.

CONCLUSIONS

The unique polycapillary optic and X-ray source in this prototype system showed definite trends in the data, and enabled the solution-mediated transformation of the metastable to the stable polymorph of flufenamic acid to be followed by XRPD during wet granulation. The online X-ray data obtained during the granulation demonstrate that polymorphic transformations during the wetting phase of granulation follow expected trends that can be modeled using established principles of mass transport and crystallization kinetics. Following the model, the extent of polymorphic conversion will be governed by the length of the granulation time. Thus, the amount of polymorph conversion during wet granulation can be predicted and controlled. Given a known polymorphic system, a sufficiently robust model may be derived from small scale XRPD data and other obtainable physical constants to anticipate the behavior of such systems on scale-up. Additionally, using advanced online monitoring techniques, such as X-ray powder diffraction, provides better data for both calibrating the model and an opportunity for real-time control of the process.

ACKNOWLEDGMENTS

The authors acknowledge the NSF/Industry/University Cooperative Research Center for Pharmaceutical Processing and the Consortium for the Advanced Manufacturing of Pharmaceuticals (CAMP) for funding this research.

REFERENCES

1. L. L. Augsburger and M. K. Vuppala. Theory of granulation. In D. M. Parikh (ed.), *The Handbook of Pharmaceutical Granulation Technology*, Marcel Dekker, New York, 1997, pp. 7–8.
2. J. Herman, J. P. Remon, N. Visavarungroj, J. B. Schwartz, and G. H. Klinger. Formation of theophylline monohydrate during the pelletisation of microcrystalline cellulose-anhydrous theophylline blends. *Int. J. Pharm.* **42**:15–18 (1988).
3. A. Bauer-Brandl. Polymorphic transitions of cimetidine during manufacture of solid dosage forms. *Int. J. Pharm.* **140**:195–206 (1996).
4. M. W. Y. Wong and A. G. Mitchell. Physicochemical characterization of a phase change produced during the wet granulation of

chlorpromazine hydrochloride and its effects on tableting. *Int. J. Pharm.* **88**:261–273 (1992).
5. M. Otsuka, H. Hasegawa, and Y. Matsuda. Effect of polymorphic forms of bulk powders on pharmaceutical properties of carbamazepine granules. *Chem. Pharm. Bull.* **47**:852–856 (1999).
6. M. L. MacCalman, K. J. Roberts, C. Kerr, and B. Hendriksen. On-line processing of pharmaceutical materials using *in situ* X-ray diffraction. *J. Appl. Crystallogr.* **28**:620–622 (1995).
7. N. Scarlett, I. Madsen, C. Manias, and D. Retallack. On-line X-Ray diffraction for quantitative phase analysis: application in the portland cement industry. *Powd. Diffraction* **16**:71–80 (2001).
8. R. Beilmann and H. Brueggemann. Quantitative XRD clinker phase analysis "A tool for process optimization and cement quality control." *Proc. Int. Conf. Cem. Microsc*. **13**:38–59 (1991).
9. G. A. Norton, R. E. Peters, and R. A. Jacobson. Feasibility of using X-Ray diffraction for on-line analysis of gypsum during wall board manufacturing. *Miner. Eng.* **8**:1069–1074 (1995).
10. A. Martin, L. Wilde, and U. Steinike. Formation and structural characterization of ammonium vanadyl phosphates prepared by solid state reactions of vanadyl(IV) phosphates in the presence of ammonia. *J. Mat. Chem.* **10**:2368–2374 (2000).
11. O. S. Morozova, O. V. Krylov, G. N. Kryukova, and L. M. Plyasova. Effect of initial nickel and iron oxide morphology on their structural transformation in CO/H_2 mixture. *Catalysis Today* **33**: 323–334 (1997).
12. A. Molenbroek and J. K. Norskov. Structure and reactivity of Ni-Au nanoparticle catalysts. *J. Phys. Chem. B.* **105**:5450–5458 (2001).
13. B. S. Clausen, L. Grabaek, G. Steffensen, P. Hansen, and H. Topsoe. A combined QEXAFS/XRD method for on-line, in situ studies of catalysts: examples of dynamic measurements of Cu-based methanol catalysts. *Catalysis Letters* **20**:23–36 (1993).
14. T. Yamanoi and H. Nakazawa. Parallel-beam X-Ray diffractometry using X-ray guide tubes. *J. Appl. Crystallogr.* **33**:389–391 (2000).
15. P. J. Schields, D. M. Gibson, W. M. Gibson, N. Gao, H. Huang, and I. Y. Ponomarev. Overview of polycapillary X-ray optics. *Powd. Diffraction* **17**:70–80 (2002).
16. J. Krc. Crystallographic properties of flufenamic acid. *Microscope* **25**:31–45 (1977).
17. S. R. Byrn, R. R. Pfeiffer, and J. G. Stowell. *Solid State Chemistry of Drugs*, 2nd ed.: SSCI Inc., West Lafayette, Indiana, 1999.
18. D. Kunii and O. Levenspiel. *Fluidization Engineering*, John Wiley & Sons, New York, 1969.
19. J. W. Mullin. *Crystallization*, 3rd ed. Butterworth-Heinemann, Oxford, 1993.
20. P. T. Cardew and R. J. Davey. The kinetics of Solvent-Mediated Phase Transformations, *Proc. Royal Soc. London. Series A. Mathematical and Physical Science* **398**:415–428 (1985).